

## **SIMPLIFIED ANALYTICAL-MECHANICAL METHODOLOGY FOR STRUCTURAL-SEISMIC SAFETY ASSESSMENT OVER TIME OF RC BRIDGES AFFECTED BY CORROSION PHENOMENA**

**M. Gentile<sup>1</sup>, F. Molaioni<sup>2</sup>, S. Pampanin<sup>1</sup>**

<sup>1</sup> Sapienza University of Rome, Department of Structural and Geotechnical Engineering  
Via Eudossiana 18, 00184, Rome, Italy  
[matteo.gentile8@gmail.com](mailto:matteo.gentile8@gmail.com), [stefano.pampanin@uniroma1.it](mailto:stefano.pampanin@uniroma1.it)

<sup>2</sup> University of Rome Tor Vergata, Dept. of Civil Engin. and Computer Science Engin. (DICII),  
Via del Politecnico 1, Rome, 00133, Italy  
[filippo.molaioni@uniroma2.it](mailto:filippo.molaioni@uniroma2.it)

---

### **Abstract**

*Existing R.C. bridge structures are generally subject to intense environmental attacks. Over time, environmental actions can trigger structural deterioration effects, the most common of which is the rebars corrosion. As steel reinforcement corrosion could reduce the capacity of R.C. members, the seismic safety of R.C. bridges could be compromised by these phenomena. In accordance with international guidelines, the initial assessment of bridges is carried out by identifying and grading defect-indices after a visual inspection of the structure. This study arises from the need to find a quantitative correlation between the grading scale adopted in the evaluation of defect-indices and the impact of corrosion effects on RC members capacity and safety, also evaluating the evolution over time of degradation. A practical simplified, whilst mechanical-based, analytical methodology for assessing the seismic safety starting from defect-index visual assessment of RC bridges subject to degradation corrosive attacks, is presented and applied to a case study RC bridge representative of the main characteristics of the viaducts of Italy. Different chloride damage scenarios related to defect-indices are considered for the piers of the case study bridge and the seismic safety of the structure is analytically evaluated. Two corrosion rate limit conditions are then considered to evaluate (upper and lower bound) effects on seismic safety over time. Finally, an estimate of the epistemic uncertainty due to the visual assessment of the damage is performed to obtain the structure collapse probability. The analytical results underline that the seismic safety is strongly influenced both by the location and the evolution of corrosion phenomena over time. By identifying the safety and collapse probability of the structures, the proposed methodology can be used as a decision-making support tool regarding the need for intervention with maintenance/restoration/retrofit solutions.*

**Keywords:** Reinforced Concrete, Bridges, Seismic Safety, Seismic Assessment, Corrosion, Collapse Probability.

## 1 INTRODUCTION

The structural-seismic safety assessment of existing reinforced concrete bridges is a long-standing key topic in civil engineer [1]. The Italian territory, characterized by medium-high seismicity, has a large stock of old RC bridge structures, typically prior to the introduction of seismic-resistant and durability principles and code provisions [2-4]. Deterioration phenomena may be triggered by aggressive environmental conditions for RC structures lacking adequate construction details. In these cases, corrosion of reinforcing rebars represents the most frequent and dangerous deterioration phenomenon. Once activated, corrosion can occur in a uniform or localized manner; uniform corrosion is caused by humid and carbon dioxide-rich environmental conditions; pitting corrosion instead activates due to the penetration of chloride ions in concrete, a frequent case for bridges due to the application of de-icing salts.

Corrosion of the steel reinforcement affects the mechanical properties of the materials, leading to reduction of the resistant section of the steel bars and of the reinforcement deformation capacity, cracking of cover concrete, and deterioration of the bond strength. In recent decades, considerable efforts have been devoted to understanding the mechanical behavior of corroded R.C. members. In Rodriguez et al. 1997 [5], Castel et al. 2000 [6], Meda et al. 2014 [7] experimental tests were carried out to evaluate flexural, shear and cyclic behavior. The effects on material properties such as stress-strain and/or bond strength laws were identified in Alonso et al. 1996 [8], Almusallam et al. 2001 [9], Apostolopoulos et al. 2008 [10], Imperatore et al. 2017 [11], FIB Model Code 2020 [12]. The reinforcing bars corrosion phenomenon is characterized by two phases [13]: the initiation phase, when atmospheric agents penetrate the concrete until the reinforcement depassivation, and the propagation phase when the impact on materials further evolve over time. Since the seismic performance of bridge structures is highly dependent on the mechanical behavior of its elements, thus on the state of decay, the assessment of seismic structural safety of existing structures and infrastructures should take into account the quantitative evaluation of capacity reduction and its impact on performance/safety due to rebars corrosion.

Given the key strategic role of bridge structures within a country's road network, and the potentially substantial socio-economic costs associated with demolition-reconstruction interventions, several national and international guidelines on the evaluation of existing reinforced concrete bridges have been issued in recent years [14,15]. The common goal is to develop practical and reliable bridge-state assessment procedure and define appropriate maintenance-retrofit solutions for degraded and unsafe structures. Some of these guidelines (e.g., [14]), provide for a multilevel (tiers) approach based on the identification of defect indices following a


Visual Inspection	Defect	Severity (G)	Extention (k1)	Intensity (k2)	Total Score
	Unidity	x	x	x	G + k1 + k2
	Concrete Deterioration	x	x	x	
	Cracking	x	x	x	
	Cover Spalling	x	x	x	
	Stirrups Corrosion	x	x	x	
	Rebars Corrosion	x	x	x	
Relative Defect Coefficient				$\sum_i G_i + k1_i + k2_i$	

Figure 1: Example of Defect Indices Datasheet

visual inspection of the structure: for each area of the bridge the defects are identified, and through "qualitative scores" the severity and extent of the defects are graded. Figure 1 shows an example on how these approaches work. The Relative Defect Coefficient (DS) is calculated from the weighted sum of the individual defects (G) multiplied by the intensity ( $k_1$ ) and extension ( $k_2$ ) coefficients. Depending on the overall scoring (DS), the codes provide procedures that may highlight the need for more in-depth investigations, aimed at verifying the effective structural capacity, or the possibility of carrying out only maintenance interventions or proceeding with the downgrading of the bridge.

In the authors' opinion, such approach, based on visual inspections, could and should be further developed using mechanical-based methodologies in order to quantitatively evaluate the potential capacity-reduction of RC structural members and, therefore, of the structures static and seismic safety.

The aim of this work is to develop and integrate a quantitative mechanical-based assessment of RC members to the visual inspection and defect indices qualitative "scoring" approach in order to suggest a methodology for structural and seismic safety assessment of deteriorated RC bridges. To achieve this goal, a practical analytical methodology [16,17,18,19,20], whilst mechanical-based, referred to as SLaMA (Simple Lateral Mechanism Analysis) is further extended to for the evaluation of the seismic performance/safety evaluation of existing bridges, specifically including considerations on the capacity assessment of corroded RC structural members. In this work, the seismic safety of a case study reinforced concrete bridge, representing an archetype of widespread bridge typologies in Italy, affected by corrosion phenomena, is evaluated. Three different degradation scenarios are considered: corrosion intensity in terms of percentage mass loss is chosen consistently with three different defect indices, defined according to [14], thus integrating a quantitative measure to the visual inspection approach. Corrosion effects on members capacity reduction are analytically calculated as reported in [11,21,22]. The global seismic capacity of the bridge is determined and therefore the safety index defined in [14] is calculated. Considering different corrosion propagation models [23,24,25,26], upper and lower bounds for corrosion rates are adopted, and the seismic safety reduction over time is assessed. The uncertainty related to the location and extent of degradation is evaluated, and finally, using a simplified probabilistic approach [27] the fragility curves associated to the bridge collapse probability are calculated as a function of the peak ground acceleration for each degradation scenario.

## 2 SLAMA-BRIDGE METHODOLOGY INCLUDING DETERIORATION EFFECTS

The proposed procedure, schematically shown in the flow-chart of Figure 2, consists of the simplified seismic assessment of existing RC bridges based on the SLaMA approach for bridges [16,17,18,19], integrated with the evaluation of element capacity reduction evaluation due to corrosion of the reinforcement bars. As a first step, the seismic capacity of the pier is calculated determining the force-displacement curve. In this phase, it is crucial to correctly identify the 'critical section' where the plastic hinge and potential associated energy dissipation is expected to occur and develop. Generally, for bridges piers the plastic hinge region is expected to be located as the base, given their cantilever scheme; however, in case of localized environmental corrosive attack, the structural deterioration can modify the structural nonlinear behavior, and consequently, the critical sections can be relocated [28].

Therefore, it is important to support such estimation on the specifically planned visual inspections of the degradation. As part of the members capacity evaluation, the interaction between flexure and shear mechanisms is taken into account by comparing the force-displacement curve and the degrading-shear capacity curve calculated according to [29].

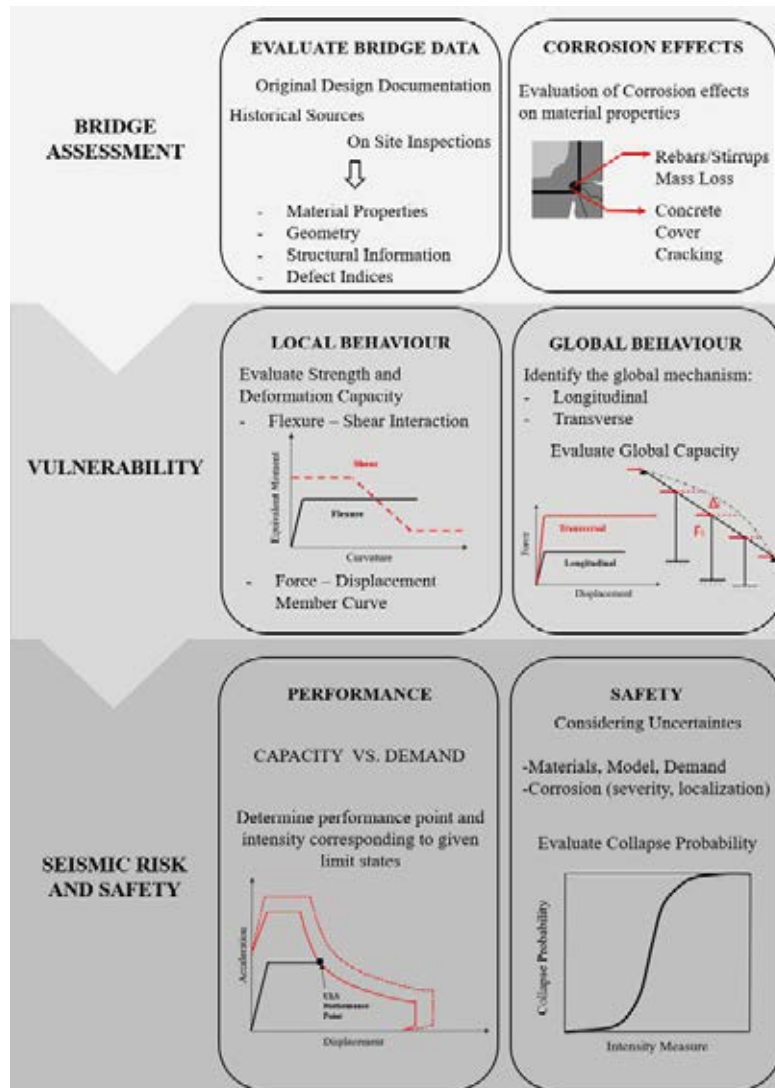


Figure 2: Methodology Flow Chart

In this paper, the evaluation of the plastic hinge length is calculated as the average value of the results related to different formulations available in the literature [30,31,32]. In a section analysis (or fiber numerical model) approach, the corrosion effect is taken into account by reducing the mechanical properties of the reinforcements as reported in [11] and by reducing the concrete cover compressive strength to consider the cracking induced by oxides expansion [33,34]. The overall seismic capacity of the bridge is evaluated separately for the longitudinal and transverse directions. The relationship between the local and global capacity is closely related to the static scheme of the bridge. The most common schemes for existing reinforced concrete bridges are continuous beam and supported beam ones. As reported in [35], in case of supported beams, and in the absence of seismic restraints, each pier behaves independently therefore, in a simplified way, the performance of the bridge is governed by the performance of the weakest (performance-wise) pier, both in longitudinal and transverse direction. On the other hand, in the case of continuous beam scheme: in the longitudinal direction, same top displacement can be assumed for all piers and the overall capacity is obtained by adding in parallel the individual

capacities of each pier; in the transverse direction, following a displacement approach presented in [36], the global capacity curve is obtained by adding the singles piers capacity in proportion to the piers effective displacement identified for the principal vibration mode of the structure. The global displacement instead is determined by referring to an equivalent SDOF. The seismic safety is measured through the safety index  $\zeta_E$  (also referred to as IS-V and %NBS in the ITA2017 and NZSEE2017 guidelines, respectively) [14, 16, 29], or Capacity/Demand ratio, obtained by comparing the bridge capacity curve with the ADRS seismic demand spectrum SLV limit state [29].

One of the objectives of this paper is the further extension of the analytical assessment methodology to account for the potential reduction of safety over time. To achieve this scope, an extensive literature review on research on the corrosion rate models available in the literature has been carried out, both for the carbonation and for the chlorides attack phenomenon. Since pitting corrosion due to chloride attack is characterized by a higher rate (Figure 3), in this work this typology is considered for the deterioration scenarios applied to the structure.

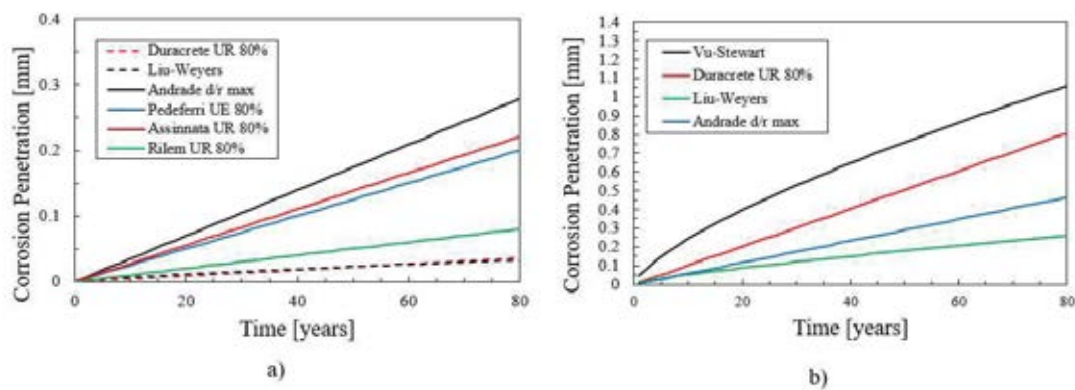


Figure 3: Corrosion rate models. a) Carbonation. b) Chlorides attack.

In the Defect Indices Approach through visual inspections, no explicit empirical or theoretical relationships are associated to the determination of the so called “extension” and “intensity” coefficients, and, at this stage, there are no quantitative correlation between the grading scale and the actual mechanical material properties reduction, making a structural mechanical assessment that takes into account deterioration phenomena not applicable.

To overcome these issues, a probabilistic approach is adopted in this work: the probability of the structure to overcome a certain damage level is determined as a function of the seismic intensity. The fragility curves can be calculated through analytical or empirical methods. In [27] most of the analytical methods adopted for buildings are presented. In [37] empirical methods are proposed for the calculation of the fragility curves according to the considered structure.

For the sake of simplicity and in the absence of more detailed data, in the simplified collapse probability assessment procedure herein proposed for a corroded reinforced concrete bridge structure, variations in the main factors affecting the corroded member capacity are considered, in particular: the location of the critical section, the amount of lost mass and the number of bars involved. Extensive analyses have been carried out varying both parameters.

In this way both corrosion location and intensity uncertainty related to the assumed deterioration scenarios are accounted and then combined, as recommended in [28], through SRSS rule with the epistemic (model and material characteristics) and aleatoric (seismic demand) uncertainties  $\beta$  value of 0.6 suggested in [37].



### 3 CASE STUDY BRIDGE

#### 3.1 Geometric and mechanical characteristics

The case study Bridge is an archetype representative of typical characteristics of a large number of R.C. bridges in the Italian territory (Figure 4). The geometry, material properties and static scheme of the bridge were selected through the analysis of a database of the Italian bridges in central Italy [20]. The database shows a strong prevalence of supported beam scheme, therefore herein selected for the case study. The bridge consists of four 30 m spans. Deck beams consist of I-shape prestressed reinforced concrete with prestressed 7-wire strands with straight longitudinal profile. The Piers have hollow polygonal section. Table 1 reports the key geometric characteristics of piers. The material mechanical properties (Table 2) have been selected as average values of the concrete cubic compressive strength and of the reinforcement yield strength values available in the database. In this regard, it is worth noting that material properties design values are obtained by reducing the mean values by partial safety factors and knowledge factor according to the Italian Code Provisions NTC2018 and associated Commentary 2019 for existing Structures and Infrastructures [14,29].

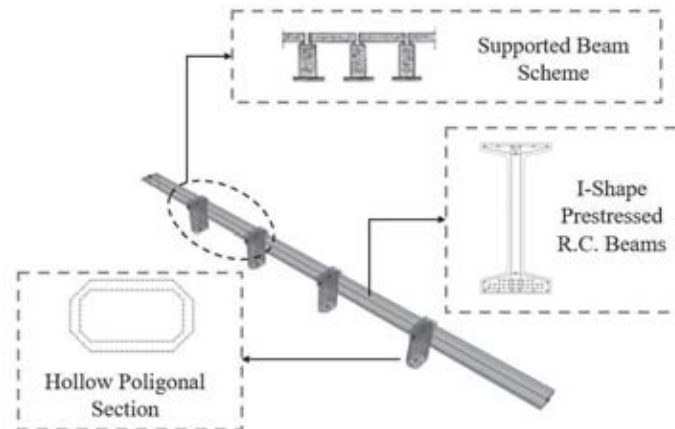


Figure 4: Archetype example for Italian Territory bridges

Pier Section	Lenght	$A_{conc}$	$\Phi_{long}$	$\rho_{long}$	$\Phi_t$	s
	[m]	[m <sup>2</sup> ]	[mm]	[%]	[mm]	[mm]
	10	7	20	0.45	10	250

Table 1: Case study piers geometry

Concrete				Steel			
$f_{cd}$	$E_{cm}$	$\epsilon_{c0}$	$\epsilon_{cu}$	$f_{yd}$	$E_s$	$\epsilon_{sy}$	$\epsilon_{su}$
[MPa]	[GPa]	[-]	[-]	[MPa]	[GPa]	[-]	[-]
26.80	29.57	0.2	0.35	375.00	210.00	0.18	6.75

Table 2: Case study piers material properties

As regards the seismic demand, conditions of high seismicity were considered. Reference is made to the L'Aquila site, representative of the seismology of central Apennine Italy. A nominal life  $V_N = 100$  years and an Importance Level IV (Important strategic functions structures) [29] are considered in order to account for the strategic function of the bridge structure. In Table 3 the main parameter of the elastic acceleration response spectrum are presented for the limit states of (Fully) Operational (SLO), Damage Control (SLD), Life Safety (SLV) and Collapse Prevention (SLC).

$P_{VR}$	$T_R$	LIMIT STATE	$a_g$	$F_0$	$T^*_C$
[-]	[years]	[-]	[g]	[-]	[s]
81%	120	SLO	0.15	2.3	0.30
63%	201	SLD	0.19	2.31	0.32
10%	1898	SLV	0.41	2.44	0.38
5%	2475	SLC	0.45	2.46	0.38

Table 3: Response spectrum parameters

Three different degradation scenarios are applied to the case study bridge in order to evaluate the potential losses in terms of seismic safety due to the corrosion effects. Each scenario, representative of a specific degradation level, is associated to the “Relative Defect Coefficient” evaluated according to the qualitative defect sheets of the Italian guidelines for the evaluation of existing bridges. In Figure 5 visual examples for assumed degradation scenarios are given.

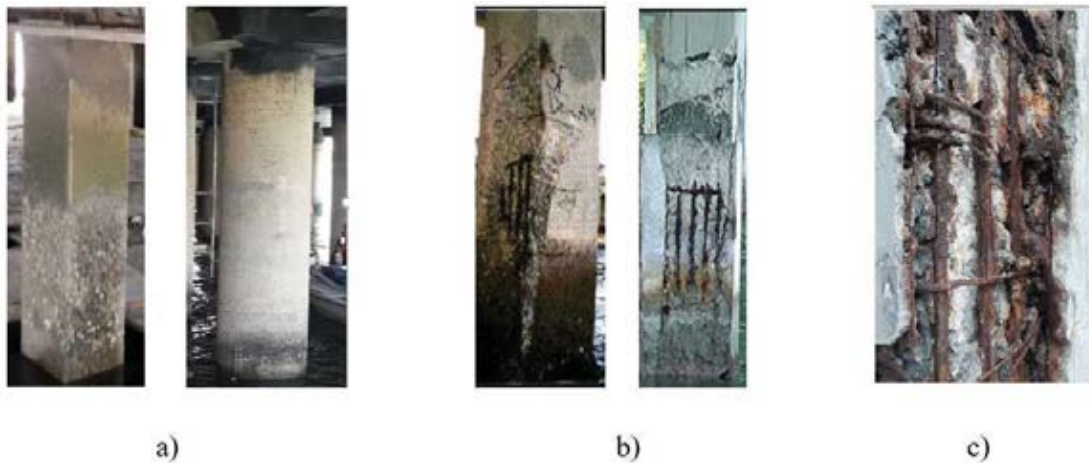


Figure 5: Examples of degradation scenarios: a) Low degradation – Scenario 1. b) Medium degradation – Scenario 2. c) High degradation – Scenario 3.

<b>Scenario 1 - Low Degradation</b>				
Defect	Severity	Extention	Intensity	Total Score
Umidity	4.00	0.50	1.00	2.00
Concrete Deterioration	2.00	0.50	1.00	1.00
Cracking	2.00	1.00	0.20	0.40
Rebars Corrosion	5.00	0.20	0.20	0.20
Relative Defect Coefficient				3.60
<b>Scenario 2 - Medium Degradation</b>				
Defect	Severity	Extention	Intensity	Total Score
Umidity	4.00	0.50	1.00	2.00
Concrete Deterioration	2.00	0.50	1.00	1.00
Cracking	2.00	1.00	1.00	2.00
Cover Spalling	2.00	0.20	1.00	0.40
Stirrups Corrosion	3.00	0.50	0.50	0.75
Rebars Corrosion	5.00	0.20	0.50	1.25
Relative Defect Coefficient				7.40
<b>Scenario 3 - High Degradation</b>				
Defect	Severity	Extention	Intensity	Total Score
Umidity	4.00	0.50	1.00	2.00
Concrete Deterioration	2.00	0.50	1.00	2.00
Cracking	2.00	1.00	1.00	2.00
Cover Spalling	2.00	0.20	1.00	2.00
Stirrups Corrosion	3.00	0.50	0.50	1.50
Rebars Corrosion	5.00	0.20	0.50	1.25
Relative Defect Coefficient				10.75

Table 4: Degradation scenarios parameters considered for the case study

In Table 4 the degradation parameters assumed for each scenario are presented. For the Scenario 1, low degradation conditions are considered: it is assumed that corrosive agents have broken the protective film of the bars but the corrosion of the latter has just begun ( $M_{\text{loss}} = 5\%$ ), the most obvious defect being the extensive deterioration of the concrete with capillary cracking. In Scenario 1, the extent of the degradation is considered localized. The position of deterioration is parametrically shifted to assess the influence of the location of the damage on the capacity of the structure. For the Scenario 2, medium degradation conditions are considered with rebars corrosion ( $M_{\text{loss}} = 15\%$ ) and partial detachment of the concrete cover. Also for Scenario 2 the extent of the deterioration is assumed localized. For the Scenario 3, severe and limit conditions are considered: rebars corrosion is high ( $M_{\text{loss}} = 25\%$ ) and the stirrups are no longer considered resistant, the concrete cover has spalled and the extent of the damage affects a large part of the pier. In Table 5 the corrosion consequences on material properties are presented for each scenario, the reinforcement mass loss values ( $M_{\text{loss}}$ ) were chosen consistently with values found in the literature for chlorides corrosion [11, 35].



	Steel					Concrete	
	$M_{loss}$	$\epsilon_{sy}$	$\epsilon_{su}$	$f_{ym}$	$f_{um}$	$w$	$f_{c,rid}$
	[-]	[-]	[-]	[Mpa]	[Mpa]	[mm]	[Mpa]
Scenario 1	5%	0.20%	5.13%	337.57	489.67	0.12	26.37
Scenario 2	15%	0.12%	2.97%	260.27	389.00	0.82	24.21
Scenario 3	25%	0.09%	1.72%	186.11	288.33	4.09	21.12

Table 5: Corrosion consequences on material properties

Given the high uncertainty of the corrosion rate, an upper and a lower bound were identified through the study of predictive models available in the literature and adopted to evaluate the reinforcement mass losses,  $M_{loss}$  for the case study bridge over a period of 15 years. The limit values of the corrosion rates together with the consequent  $M_{loss}$  values assumed over time are shown in Figure 6.

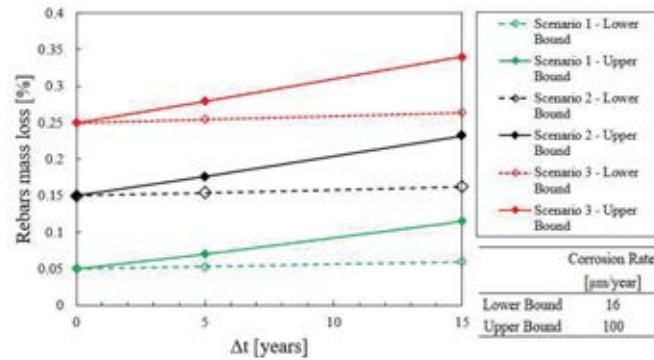


Figure 6: Corrosion intensity evolution for each scenario: a) Lower bound corrosion rate. b) Upper bound corrosion rate

### 3.2 Safety reduction and risk assessment results

The models described above for the strength and ductility losses for structural members subject to corrosion were applied to the structure for the three deterioration scenarios. Figure 7 shows the moment-curvature curve for the weakest bridge pier for the non-corroded case and each corrosion scenario considered. It can be noted that as the degradation increases, a marked loss of element ductility is observed. This effect is mainly due to the reduction in terms of steel ultimate deformation capacity.

Then the bridge seismic capacity for each scenario was calculated. In Figure 8 the global capacity curves and expected performance within a ADRS (Acceleration Displacement Response Spectrum) domain are presented for the longitudinal direction. Worth noting that, as the seismic safety in the transverse direction did not present significant problems for any scenario, albeit with a reduction in vulnerability, the results have been herein omitted. As it can be observed, in the longitudinal direction the seismic safety check is no longer satisfied for all scenarios. The safety index reduces from  $\zeta_e=1.15$  for the non-corroded case to a  $\zeta_e=0.98$ , 0.71 and 0.61, for scenario 1, 2 and 3.

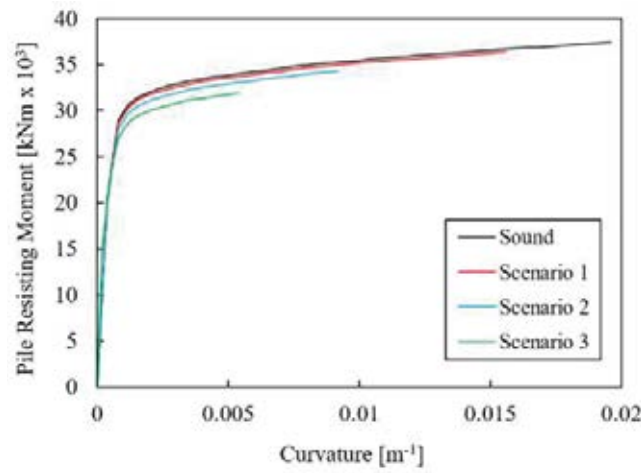


Figure 7: Moment-curvature relationship for the base section of bridge piers

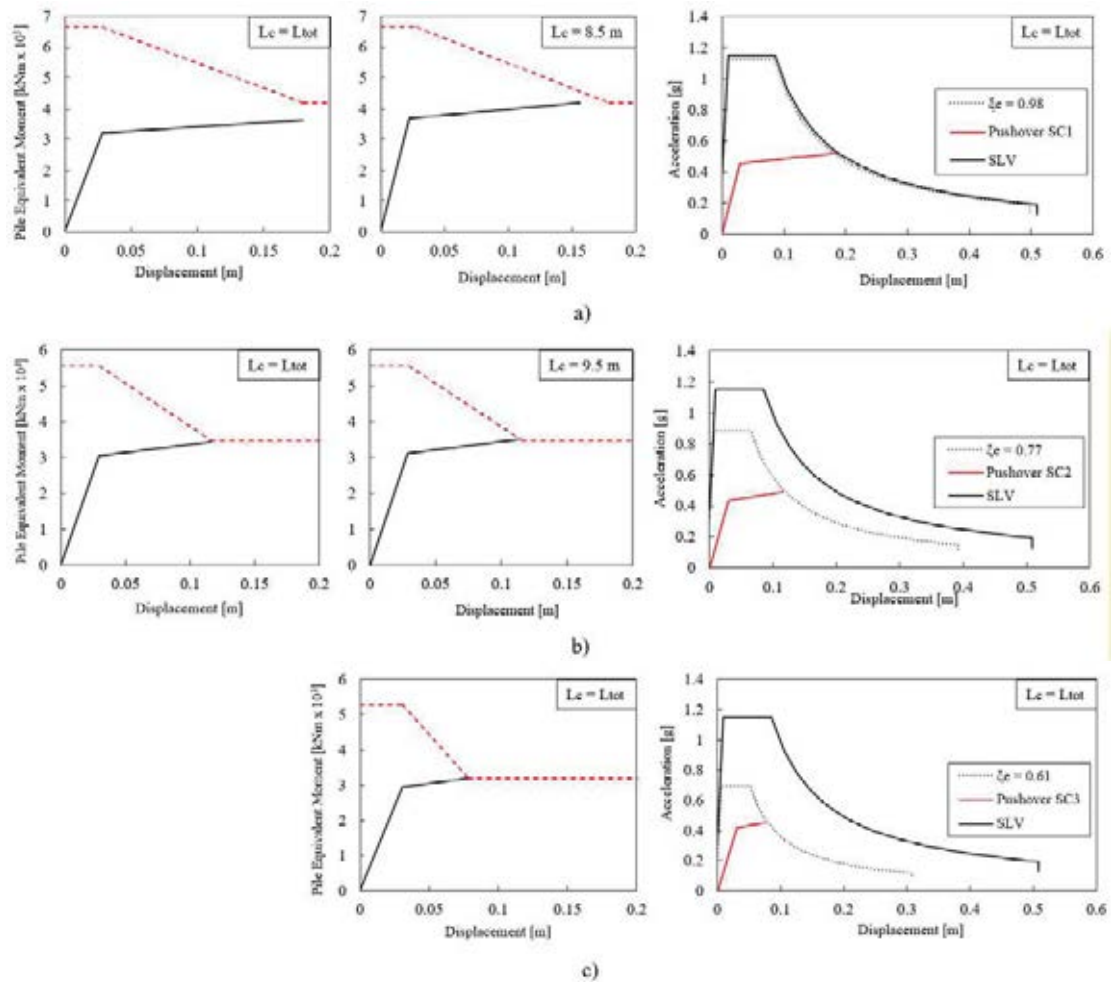


Figure 8: Capacity curves and safety index evaluation for the case study bridge. a) scenario 1. b) scenario 2. c) scenario 3.

Considering the upper and lower bound corrosion rate values previously described, the decay of the Safety Risk index over time is evaluated and shown in Figure 9. For the case study, a maximum percentage loss of seismic safety in 15 years of about 47% for scenario 3 is assessed. Reduction due to the upper bound corrosion rate in 15 years is about 15%, while for the lower bound is about 2.5% highlighting the extreme importance of this parameter characterized by high uncertainty.

In order to calculate the collapse probability of piers, variations in the intensity (3-30%  $M_{loss}$ ), in the number of corroded bars, in the critical damaged section location (base section, 0.25L, 0.5L) are considered. Altogether a sample of 186 performance data of the structure referred to the achievement of the ultimate displacement of the pile is obtained. The reference parameter is the PGA, peak ground acceleration, associated with a given damage state. The damage states considered are the displacement limits reported in the study in [39]. For the Collapse Prevention limit state the displacement limit considered is the ultimate one. The values obtained for the corrosion localization and damage uncertainties and the combination of the two with the epistemic and aleatoric uncertainties are reported in Table 6.

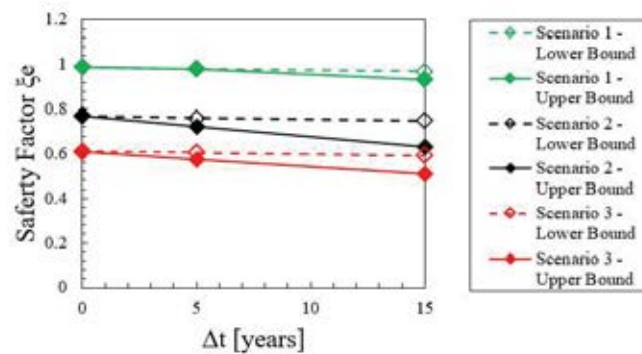


Figure 9: Safety factor decay over time due to corrosion development

	PGA [g]	$\beta_{\text{model+materials+demand}}$ [-]	$\beta_{\text{localization}}$ [-]	$\beta_{\text{damage}}$ [-]	$\beta_{\text{localization+damage}}$ [-]	$\beta_{\text{total}}$ [-]
Sound	0.43	0.6	-	-	-	0.6
Scenario 1	0.4	0.6	0.17	0.16	0.24	0.65
Scenario 2	0.35	0.6	0.17	0.16	0.24	0.65
Scenario 3	0.31	0.6	0.17	0.16	0.24	0.65

Table 6: Main parameters for fragility curves calculation

The collapse probability curves were then calculated for the non-corroded bridge and each scenario considered. The results are reported in Figure 10. As the severity of the deterioration increases, the fragility curve shifts to the left. This indicates that, as expected, as the damage from deterioration increases, there is a greater probability of collapse for a given PGA (seismic intensity).

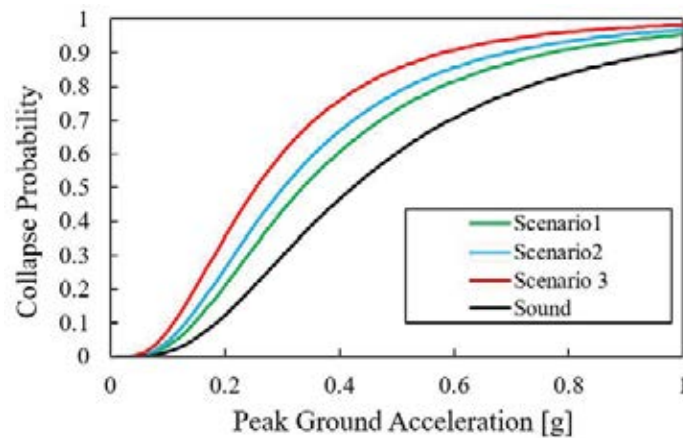


Figure 10: Collapse probability - Pier

#### 4 CONCLUSIONS

In this work, a practical methodology for the seismic safety assessment of reinforced concrete bridges subject to corrosion phenomena was presented. Furthermore, considering different corrosion propagation models, seismic safety losses were also evaluated over time. The methodology was applied to a case study bridge (archetype), representative of the most typical technology and structural scheme adopted in the Central Italy territory. Finally, considering the epistemic and aleatoric uncertainties related to the materials, to the model, to the seismic demand, and to the corrosion intensity and localization starting from a defect index, the methodology allows to calculate the collapse probability curves, considering the ultimate displacement of the piers as Engineer Demand Parameter and the PGA taken as Intensity Measure.

The assessment results of the case study show that for bridges with supported beam static scheme the sensitivity to corrosion phenomena may significantly undermine the structure seismic safety. For the most severe deterioration scenario, results in terms of safety factor and fragility curve show the need for retrofit intervention to recover the initial safety level. Results obtained for the mild and medium intensity scenarios, on the other hand, do not seem to cause immediate and significant reductions in safety. Yet the study of the evolution of corrosive phenomena over time shows that, in the case of high corrosion rates, safety may be compromised within a few years. For these cases it should also be considered that time can cause the deterioration to evolve not only in intensity but also in extension, thus potentially moving in a short time into a more severe deterioration scenario. In these cases, therefore, although structural restoration interventions might not be urgent, continuous monitoring and appropriate maintenance plans including preventive “light” restoration interventions might be critical to preserve the integrity and safety of the bridge in the long-term.

The analyses carried out show a significant loss of capacity in the case of localization of a weak section along the height of the pier rather than at the base.

The methodology presented, both for its simplicity and its effectiveness can represent a useful support tool integrating the visual inspection approach for assessing the corrosion effects on the R.C. bridge piers and therefore evaluating the overall structure seismic capacity. It can, therefore, represents a valuable decision support tool in terms of retrofit/restoration/maintenance

priorities related to the seismic performance of the structure. Further improvement and refinement of the methodology are needed and are under developments, to include further sources of material deterioration as well as local and global failure mechanisms.

Yet, in the authors' opinion, the high uncertainty associated with the corrosion phenomena, both in terms of mechanical consequences and in evolution over time, remains the main issue in the evaluation of seismic capacity. In this regard, the fragility curves evaluated through the proposed methodology can somehow account for this lack of current knowledge in the form of aleatoric and epistemic uncertainties. In any case, an adequate integration of the various approaches, e.g. visual inspection, theoretical quantitative evaluation and mechanical on-site testing, within a unified framework and assessment procedure can lead to a robust hybrid procedure for a more reliable estimation and control of the static (and seismic) performance and safety of bridge structures.



## REFERENCES

- [1] Kawashima, K. (2000). Seismic design and retrofit of bridges. *Bulletin of the New Zealand Society for Earthquake Engineering*. <https://doi.org/10.5459/bnzsee.33.3.265-285>
- [2] Kumar, R., & Gardoni, P. (2014). Effect of seismic degradation on the fragility of reinforced concrete bridges. *Engineering Structures*. <https://doi.org/10.1016/j.engstruct.2014.08.019>
- [3] Mele, M., & Siviero, E. (1991). On the durability of reinforced and prestressed concrete structures. In *Courses and Lectures - International Centre for Mechanical Sciences*. [https://doi.org/10.1007/978-3-7091-2614-1\\_7](https://doi.org/10.1007/978-3-7091-2614-1_7)
- [4] Siemes, T., & Vries, H. De. (2002). *Overview Of The Development Of Service Life Design For Concrete Structures*. 1–10.
- [5] Rodriguez, J., Ortega, L. M., & Casal, J. (1997). Load carrying capacity of concrete structures with corroded reinforcement. *Construction and Building Materials*, 11(4), 239–248. [https://doi.org/10.1016/S0950-0618\(97\)00043-3](https://doi.org/10.1016/S0950-0618(97)00043-3)
- [6] Castel, A., François, R., & Arliguie, G. (2000). Mechanical behaviour of corroded reinforced concrete beams - Part 1: experimental study of corroded beams. *Materials and Structures/Materiaux et Constructions*, 33(233), 539–544.
- [7] Meda, A., Mostosi, S., Rinaldi, Z., & Riva, P. (2014). Experimental evaluation of the corrosion influence on the cyclic behaviour of RC columns. *Engineering Structures*, 76, 112–123. <https://doi.org/10.1016/j.engstruct.2014.06.043>
- [8] Alonso, C., Andrade, C., Rodriguez, J., & Diez, J. M. (1996). Factors controlling cracking of concrete affected by reinforcement corrosion. *Materials and Structures/Materiaux et Constructions*.
- [9] Almusallam, A. A. (2001). Effect of degree of corrosion on the properties of reinforcing steel bars. *Construction and Building Materials*, 15(8), 361–368. [https://doi.org/10.1016/S0950-0618\(01\)00009-5](https://doi.org/10.1016/S0950-0618(01)00009-5)
- [10] Apostolopoulos, C. A., & Papadakis, V. G. (2008). Consequences of steel corrosion on the ductility properties of reinforcement bar. *Construction and Building Materials*, 22(12), 2316–2324. <https://doi.org/10.1016/j.conbuildmat.2007.10.006>
- [11] Imperatore, S., Rinaldi, Z., & Drago, C. (2017). Degradation relationships for the mechanical properties of corroded steel rebars. *Construction and Building Materials*, 148, 219–230. <https://doi.org/10.1016/j.conbuildmat.2017.04.209>
- [12] fib Model Code 2020 . (2019). *Structural Concrete*. <https://doi.org/10.1002/suco.201970021>
- [13] Tuutti, K. (1977). CORROSION OF STEEL IN CONCRETE. *EUROCOR '77, Eur Congr on Met Corros, 92nd Event of the Eur Fed of Corros*, 655–661.
- [14] Ministero delle Infrastrutture e dei Trasporti. (2019). Linee Guida per la Classificazione e Gestione del Rischio, la Valutazione della Sicurezza ed il Monitoraggio dei ponti esistenti, allegate al parere del CSLPP n.88/2019.
- [15] FHWA. (1971). National Bridge Inspection Standards. *Federal Register*.

- [16] NZSEE (2017). New Zealand Society for Earthquake Engineering. The seismic assessment of existing buildings – technical guidelines for engineering assessments. Wellington, New Zealand;
- [17] Pampanin, S., (2017) Towards the practical implementation of performance-based assessment and retrofit strategies for RC buildings: challenges and solutions, SMAR2017-Fourth conference on Smart Monitoring, Assessment and Rehabilitation of Structures, *Keynote Lecture*, 13-15 Sept, Zurich, Switzerland
- [18] Del Vecchio, C., Gentile, R. & Pampanin, S. (2017) The Simple Lateral Mechanism Analysis (SLaMA) for the seismic performance assessment of a case study building damaged in the 2011 Christchurch earthquake, *Research Report* N. 2016-02, University of Canterbury, Christchurch, New Zealand
- [19] Rotatori, R.M., (2019) “Valutazione della Vulnerabilità Sismica e Strategie di Miglioramento dei Viadotti a Travata in Calcestruzzo Precompresso attraverso la procedura SLaMa”, Laurea Magistrale (ME) Thesis (Supervisors: Prof. Ing. Stefano Pampanin and Prof. Ing. Fabio Brancaleoni), Department of Structural and Geotechnical Engineering, Sapienza University of Rome
- [20] Gentile, R., Nettis, A., & Raffaele, D. (2020). Effectiveness of the displacement-based seismic performance assessment for continuous RC bridges and proposed extensions. *Engineering Structures*. <https://doi.org/10.1016/j.engstruct.2020.110910>
- [21] Jeon, C. H., Lee, J. Bin, Lon, S., & Shim, C. S. (2019). Equivalent material model of corroded prestressing steel strand. *Journal of Materials Research and Technology*. <https://doi.org/10.1016/j.jmrt.2019.02.010>
- [22] Coronelli, D., & Gambarova, P. (2004). Structural Assessment of Corroded Reinforced Concrete Beams: Modeling Guidelines. *Journal of Structural Engineering*. [https://doi.org/10.1061/\(asce\)0733-9445\(2004\)130:8\(1214\)](https://doi.org/10.1061/(asce)0733-9445(2004)130:8(1214))
- [23] DuraCrete. (1998). *Modelling of degradation*, The European Union – Brite EuRam III.
- [24] Andrade, C., Alonso, C., & Sarfa, J. (2002). Corrosion rate evolution in concrete structures exposed to the atmosphere. *Cement and Concrete Composites*. [https://doi.org/10.1016/S0958-9465\(01\)00026-9](https://doi.org/10.1016/S0958-9465(01)00026-9)
- [25] Liu, T., & Weyers, R. W. (1998). Modeling the dynamic corrosion process in chloride contaminated concrete structures. *Cement and Concrete Research*. [https://doi.org/10.1016/S0008-8846\(98\)00259-2](https://doi.org/10.1016/S0008-8846(98)00259-2)
- [26] Vu, K. A. T., & Stewart, M. G. (2000). Structural reliability of concrete bridges including improved chloride-induced corrosion models. *Structural Safety*. [https://doi.org/10.1016/S0167-4730\(00\)00018-7](https://doi.org/10.1016/S0167-4730(00)00018-7)
- [27] FEMA. (2018). FEMA P-58-1: Seismic Performance Assessment of Buildings. Volume 1 – Methodology. *Fema P-58*.
- [28] Yuan, W., Guo, A., & Li, H. (2017). Seismic failure mode of coastal bridge piers considering the effects of corrosion-induced damage. *Soil Dynamics and Earthquake Engineering*. <https://doi.org/10.1016/j.soildyn.2016.12.002>
- [29] NTC, I. M. of I. and. (2018). Norme Tecniche per le Costruzioni. DM 17/1/2018. *Gazzetta Ufficiale Della Repubblica Italiana*.

- [30] Berry, M. P., Lehman, D. E., & Lowes, L. N. (2008). Lumped-plasticity models for performance simulation of bridge columns. *ACI Structural Journal*. <https://doi.org/10.14359/19786>
- [31] Panagiotakos, T. B., & Fardis, M. N. (2001). Deformations of reinforced concrete members at yielding and ultimate. *ACI Structural Journal*. <https://doi.org/10.14359/10181>
- [32] Priestley, M. J. N., & Park, R. (1987). STRENGTH OF DUCTILITY OF CONCRETE BRIDGE COLUMNS UNDER SEISMIC LOADING. *ACI Structural Journal*. <https://doi.org/10.14359/2800>
- [33] Coronelli, D., & Gambarova, P. (2004). Structural Assessment of Corroded Reinforced Concrete Beams: Modeling Guidelines. *Journal of Structural Engineering*. [https://doi.org/10.1061/\(asce\)0733-9445\(2004\)130:8\(1214\)](https://doi.org/10.1061/(asce)0733-9445(2004)130:8(1214))
- [34] Vecchio, F. J., & Collins, M. P. (1986). MODIFIED COMPRESSION-FIELD THEORY FOR REINFORCED CONCRETE ELEMENTS SUBJECTED TO SHEAR. *Journal of the American Concrete Institute*.
- [35] Progetto DPC-Reluis. (2009). *Linee guida e manuale applicativo per la valutazione della sicurezza sismica e il consolidamento dei ponti in c.a.*
- [36] Dwairi, H., & Kowalsky, M. (2006). Implementation of inelastic displacement patterns in direct displacement-based design of continuous bridge structures. *Earthquake Spectra*. <https://doi.org/10.1193/1.2220577>
- [37] FEMA, F. E. M. A. (2015). Hazus–MH 2.1: Technical Manual. *National Institute of Building Sciences and Federal Emergency Management Agency (NIBS and FEMA)*.
- [38] Dai, L., Wang, L., Bian, H., Zhang, J., Zhang, X., & Ma, Y. (2019). Flexural Capacity Prediction of Corroded Prestressed Concrete Beams Incorporating Bond Degradation. *Journal of Aerospace Engineering*. [https://doi.org/10.1061/\(asce\)as.1943-5525.0001022](https://doi.org/10.1061/(asce)as.1943-5525.0001022)
- [39] Cardone, D. (2014). Displacement limits and performance displacement profiles in support of direct displacement-based seismic assessment of bridges. *Earthquake Engineering and Structural Dynamics*. <https://doi.org/10.1002/eqe.2396>